DMD Fast Forward. Published on October 25, 2007 as doi:10.1124/dmd.107.017434

DMD #17434

In Vitro P-glycoprotein Assays to Predict the in Vivo Interactions of P-glycoprotein with Drugs in the Central Nervous System

Bo Feng, Jessica B. Mills, Ralph E. Davidson, Rouchelle J. Mireles, John S. Janiszewski, Matthew D.Troutman, Sonia M. de Morais

Pharmacokinetics, Dynamics, and Metabolism Department, Pfizer Global Research and Development, Groton, CT 06340, USA

Running title: *In vitro* assays to assess the *in vivo* effect of P-gp on CNS drugs

Corresponding author: Bo Feng

Pfizer Inc., Eastern Point Road MS 8118W-131, Groton, CT 06340

Telephone: 8607152756, Email: bo.feng2@pfizer.com

Number of text pages: 22, Number of tables: 4, Number of figures: 3, Number of references: 23, Number of words in the abstract: 250, Number of words in the introduction: 991, Number of words in the discussion: 2097

Abbreviations: MDR1/Mdr1a, multi-drug resistance protein; P-gp, P-glycoprotein; CNS, central nervous system; LC/MS/MS, liquid chromatography with tandem mass spectrometry; KO, knockout; WT, wild type; BBB, blood-brain barrier; PAMPA, parallel artificial membrane permeation assay; MDCK, Madine-Darby canine kidney; MDR1-MDCK, MDR1-transfected MDCK cells; Mdr1a-MDCK, Mdr1a-transfected MDCK; B/P, brain-to-plasma ratio; K_m, apparent affinity; P_{app}, apparent permeability; $P_{appA>B}$, P_{app} determined in apical (A)-to-basolateral (B) transport direction; $P_{appB>A}$, P_{app} determined in B-to-A transport direction; ER: efflux ratio ($P_{appB>A}$ / $P_{appA>B}$); ER_{wt}: ER in MDCK wild type cells; $ER_{transfected}$: ER in transporter transfected MDCK cells; RR: ratio of ratios; RR_{MDR1}: ER in MDR1-MDCK divided by ER in wild type MDCK cells; RR_{Mdr1a}: ER in Mdr1a-MDCK divided by ER in wide type MDCK cells. AUC, area under curve; FBS, fetal bovine serum.

Abstract

Thirty-one structurally diverse marketed central nervous system (CNS)-active drugs, one active metabolite, and seven non-CNS-active compounds were tested in three P-glycoprotein (P-gp) *in vitro* assays: transwell assays using MDCK, human MDR1-MDCK and mouse Mdr1a-MDCK cells, ATPase, and Calcein AM inhibition. Additionally, the permeability for these compounds was measured in two *in vitro* models: PAMPA and apical-to-basolateral apparent permeability in MDCK. The exposure of the same set of compounds in brain and plasma was measured in P-gp knockout (KO) and wild type (WT) mice after subcutaneous administration (Doran et al., 2005). One drug and its metabolite, risperidone and 9-hydroxyrisperidone, of the thirty-two CNS compounds, and six of the seven non-CNS drugs were determined to have positive efflux using ratio of ratios (RR) in MDR1-MDCK vs. MDCK transwell assays. Data from transwell studies correlated well with the brain-to-plasma AUC ratios between P-gp KO and WT mice for the thirty-two CNS compounds. In addition, 3300 Pfizer compounds were tested in MDR1-MDCK and Mdr1a-MDCK transwell assays, with a good correlation (R^2 = 0.92) between the efflux ratios in human MDR1-MDCK and mouse Mdr1a-MDCK. Permeability data showed that the majority of the thirty-two CNS compounds have moderate to high passive permeability. This work has demonstrated that *in vitro* transporter assays help understand the role P-gp-mediated efflux activity in determining the disposition of CNS drugs *in vivo*, and the transwell assay is a valuable *in vitro* assay to evaluate human P-gp interaction with compounds for assessing brain penetration of new chemical entities to treat CNS disorders.

DMD Fast Forward. Published on October 25, 2007 as DOI: 10.1124/dmd.107.017434
This article has not been copyedited and formatted. The final version may differ from this version.

Human P-glycoprotein (P-gp, MDR1) is known as a determinant of drug absorption, distribution, and excretion of a number of clinically important drugs (Ambudkar et al., 1999; Fromm, 2000). P-gp is widely expressed in major organs, and more specifically, P-gp is highly expressed in the capillaries of blood brain barrier (BBB) and poses a barrier to brain penetration of its substrates (Schinkel, 1999). Provided that P-gp efflux liability can be a major hurdle for CNS therapeutic drugs to cross the BBB and reach the target, the interactions of CNS compounds with P-gp may lead to the lack of CNS activity due to the decreased brain penetration. Thus, the prediction and understanding of the relevance of P-gp-mediated efflux transport has become an important activity in the discovery and development of CNS drugs. In attempts to predict the effects of P-gp *in vivo*, a variety of *in vitro* P-gp assays have been developed to classify compounds as P-gp substrates. For instance, transwell-based assays using polarized cell lines such as Madin-Darby canine kidney (MDCK) cell line. The MDCK cell line can be stably transfected with human MDR1 or mouse Mdr1a, MDR1-MDCK or Mdr1a-MDCK, respectively. Comparison of the efflux ratios between MDR1-MDCK and MDCK transwell assays can provide a measure of the specific human P-gp-mediated efflux activity (Polli et al., 2001). Another widely used P-gp *in vitro* assay is the P-gp ATPase assay for assessing drugs with P-gp interactions as substrates (Sarkadi et al., 1992; Ramachandra et al., 1998). The principal reagent of the ATPase assay is a membrane preparation from insect cells highly expressing human P-gp, and functional human P-gp will transport P-gp substrates across the membrane with resulting in the release of inorganic phosphates (Scarborough, 1995; Litman et al., 1997). Finally, the *in vitro* Calcein AM P-gp inhibition assay can be used to detect compounds that inhibit P-

gp-mediated efflux of the fluorescent P-gp substrate, Calcein. The assay can differentiate P-gp inhibitors from non-inhibitors by measuring the fluorescence of Calcein (Liminga et al., 1994; Tiberghien and Loor, 1996). However, it is important to note that the Calcein AM assay is a P-gp inhibition assay, and not a substrate assay, and that P-gp substrates do not necessarily correlate with P-gp inhibitors.

In addition to P-gp *in vitro* assays, animal models have been used to assess the impact of P-gp on substrate pharmacokinetics in humans. Comparison of the brain-to-plasma (B/P) exposure ratios in Mdr1a/Mdr1b KO mice versus WT mice has become a standard experimental approach to determine whether P-gp-mediated efflux poses a potential threat to the activity of CNS agents *in vivo* (Schinkel et al., 1996). Such *in vivo* data can be used in concert with data obtained using *in vitro* models to assess the potential liability of P-gp-mediated efflux on brain exposure of compounds in humans.

Despite of all the efforts to develop *in vitro* assays to predict P-gp effects *in vivo*, a clear guidance and rationale around selection of models to aid in the CNS drug discovery and development has been limited. Towards the pursuit of selecting appropriate *in vitro* P-gp assays to support drug discovery efforts, we have identified successful CNS drugs to provide relevant context for the interpretation of preclinical P-gp models. As such, the P-gp interaction of a set of CNS and non-CNS drugs were evaluated in a battery of *in vitro* P-gp screening assays which were readily available and facile to perform. The data from the *in vitro* studies was compared to brain exposure determined *in vivo* using P-gp KO and WT mice as described by Doran et al., 2005 to assess the concordance of the *in vitro* data to the *in vivo* data. The objectives of drug selection were to identify a representative and diverse sampling of the most commonly

used CNS therapeutic agents. Thirty-one CNS drugs, and one active metabolite of a CNS drug, were selected according to sales, number of prescriptions, structural diversity, availability, pharmacology and analytical feasibility (Doran et al., 2005). The CNS drugs selected represented a number of different therapeutic indications including antidepressants, sedatives, anxiolytics, tranquilizers, anticonvulsants, etc., in which twenty-three were bases, seven were neutrals and two were acids. The detailed rationale about compound selection for the study was referenced in Doran et al., 2005. Seven non-CNS drugs were selected as controls for their consideration as P-gp modulators, although not necessarily as substrates for P-gp. Additionally, since the key concern of using these mouse models as tools to predict relevance to humans is the potential species differences that may be seen between human MDR1 and mouse Mdr1a/1b, we have performed a correlation analysis of efflux results determined in transwell assays using MDR1-MDCK and Mdr1a-MDCK cells for 3300 Pfizer compounds.

In addition to the specific interaction with P-gp, it is known that the CNS penetration of a compound is dependent on its permeability as well. Although much effort has been devoted to understand the complex relationship between the two parameters, the role that each plays in CNS penetration is not yet well established. The permeability of the 32 compounds was determined using two *in vitro* permeability assays: parallel artificial membrane permeation assay (PAMPA), and apical-to-basolateral (A>B) apparent permeability (P_{app}) in MDCK. PAMPA is a model specifically designed to measure passive membrane permeability, which is energy independent (Avdeef and Testa, 2002; Kansy et al., 1998; Kerns, 2001, Sugano et al., 2001; Wohnsland and Faller, 2001). Transport determined using MDCK cell monolayers

approximates passive biological permeability, as the MDCK cells typically show low endogenous transporter activity.

The main goal of these studies was to evaluate the *in vitro* P-gp and permeability assays to find appropriate strategies for profiling new chemical entities for P-gp efflux liability relating to the distribution of drugs in the CNS. Additional insight is given regarding the strategies for effective utilization of the *in vitro* tools available to assess P-gp efflux and the utility of various permeability assays. Finally, we report the important findings regarding the correlation of human MDR1-MDCK and mouse Mdr1a-MDCK assay results.

Materials and Methods

Chemicals and Drug Selections. The thirty-one CNS drugs, one active metabolite of a marketed CNS drug, and seven non-CNS drugs, which were tested in the *in vitro* P-gp transporter assays and permeability assays, were part of the thirty-four CNS compounds and eight non-CNS drugs used in the publication of Doran et al., 2005. The suppliers of chemicals were the same as described in Doran et al., 2005.

Materials. The WT MDCK and human MDR1-transfected MDCK cell line were acquired externally (Piet Borst, Netherlands Cancer Institute) and the murine Mdr1a-transfected MDCK cell line was constructed internally (Pfizer Inc., Groton, CT). PAMPA lipid used for PAMPA studies (4% dioleylphosphotidylcholine with 2% steric acid in Dodecane) was prepared by Avanti Polar Lipids (Alabaster, AL). High throughput screening 96-multiwell insert system, cell culture plates with polyethylene terepthalate (PET) membrane, 0.0625 cm^2 growth area, and 1 μm pore size, 96-well angled bottom collection plate without lid (non-sterile in 23 packs), T-flasks (175 cm^2), and velocity V11 peelable seal were purchased from Falcon/BD (Bedford, MA). PAMPA permeability insert plates with PVDF membranes (0.45 μm pore size) and associated labware used for PAMPA assay was obtained from Millipore (Danvers, MA). Cell culture reagents, transport buffer used for PAMPA and transwell assays (Hank's balanced salt solution with 10 mM HEPES and 25 mM D-glucose, 1.25 mM $CaCl_2$ and 0.5 mM $MgCl_2$) and cell culture reagents were purchased from Invitrogen (Gibco Laboratories, Grand Island, NY).

Methods.

DMD Fast Forward. Published on October 25, 2007 as DOI: 10.1124/dmd.107.017434
This article has not been copyedited and formatted. The final version may differ from this version.

Sample Handling. Each compound was weighed out in duplicate on 96-well master plates and solubilized in DMSO. Daughter plates were made for each screen, and compounds were run according to the typical assay protocols as described in the following text.

MDCK Cell Culture. The following procedures were used to culture MDCK and the transfected MDCK cells. The cells were grown in minimum essential medium α (MEMα) with supplements (growth media) at 37^0C, 5% CO_2 and 95% humidity. The cells were harvested using trypsin and plated at a density of $2x10^6$ cells/cm^2 in Falcon/BD 96-well insert plates with a 2 μm pore PET filter. Seeded inserts were then placed into pre-filled Falcon/BD feeder trays containing 37 ml complete growth media. The plates were incubated at 37^0C with 95% humidity and 5% CO_2 for 4 days and subsequently used for assays.

Transwell Assay Procedures. The following procedures were used for all studies performed to determine compound P_{app} using MDCK, MDR1-MDCK and Md1a-MDCK cells. All transwell assays were performed with transport buffer (Hank's balanced salt solution with 10 mM HEPES and 25 mM D-glucose, 1.25 mM $CaCl_2$ and 0.5 mM $MgCl_2$) at pH 7.4 (buffered with 10 mM HEPES). Assays were performed with 2 μM of compound (30 mM DMSO stock solution diluted in transport buffer) in duplicate. Transport studies were performed by adding compounds in transport buffer to donor well and measuring appearance in receiver well following a 5 h incubation at 37°C. For A>B transport, donor is A compartment and receiver is B compartment. For B>A transport, donor is B compartment and receiver is A compartment. Following the 5 h incubation period, samples were collected from the receiver compartment and from the original

compound in transport buffer solution, and retained for analysis. For A>B transport studies, receiver compartments were additionally washed with acetonitrile and this wash was added to the receiver sample to recover potentially non-specifically bound compound.

PAMPA Assay Procedures. PAMPA studies were conducted using the transport buffer at pH 6.5 (buffered with 10 mM MES). Assays were performed with 10 μM compound (1 mM DMSO stock diluted in pH 6.5 transport buffer) in duplicate. The PAMPA experiment was performed by adding 5 μL PAMPA lipid to the PAMPA permeability insert plate to make the PAMPA membrane. Compound was added to donor compartment, and PAMPA insert and receiver plate were incubated at 30°C for 2 h. Samples were taken from donor (initial and final time) and receiver (final time), and retained for analysis.

Transwell and PAMPA Assay Sample Analysis. Samples were analyzed using LC/MS/MS. Briefly, 25 μL of sample was injected via Gilson 215 (Gilson, Middleton, WI) or custom designed dual arm auto-sampler into an HPLC system consists of a pair of OPTI-LYNX 1X15 mm cartridge style columns custom packed with a Showa-Denko ODP polymeric material with 20 μm particle size. The system utilized a 10 port 2-position Valco switching valve (Valco Instrument Co. Inc, Houston, TX). The aqueous mobile phase was 98% 2 mM ammonium acetate/2% 50/50 (acetonitrile/methanol). The organic mobile phase was 10% 2 mM ammonium acetate/90% 50/50 (acetonitrile/methanol). Flow rates were maintained at 2 mL/minute using Jasco pumps. Detection and analysis was performed on a SCIEX API 3000 triple quadrupole mass spectrometer (Applied Biosystems Inc., Foster City, CA), operated in either positive or

DMD Fast Forward. Published on October 25, 2007 as DOI: 10.1124/dmd.107.017434
This article has not been copyedited and formatted. The final version may differ from this version.

negative ion mode. The effluent from the HPLC column was directly introduced into the Turboionspray source. Analytes and IS responses were measured using multiple reaction monitoring (MRM). The MRM for the internal standard was 687.3/319.7 for positive ion mode, or 685.3/366.1 for negative ion mode, and MRMs for the screen compounds were previously determined.

Transwell Data Analysis. The P_{app} was calculated using equation 1:

$$P_{app} = \frac{1}{Area * C_D(0)} * \frac{dM_r}{dt} \qquad 1$$

where Area is the surface area of the cell monolayer (0.0625 cm^2), $C_D(0)$ is the initial concentration of compound applied to the donor chamber, t is time, M_r is the mass of compound appearing in the receiver compartment as a function of time, and dM_r/dt is the flux of the compound across the cell monolayer. The efflux ratio (ER) was calculated using equation 2:

$$ER = \frac{P_{app,B>A}}{P_{app,A>B}} \qquad 2$$

Where A>B and B>A denote transport direction in which P_{app} was determined. The ratio of ratios (RR) was calculated using equation 3:

$$RR = \frac{ER_{transfected}}{ER_{wt}} \qquad 3$$

Where $ER_{transfected}$ is the ER determined in the transfected MDCK cells (MDR1-MDCK or Mdr1a-MDCK) and ER_{wt} is the ER determined in WT MDCK cells. The RR_{MDR1} and RR_{Mdr1a} denote RR determined for ER in MDR1-MDCK transfected cells and Mdr1a-MDCK transfected cells, respectively, compared with ER in WT MDCK.

DMD Fast Forward. Published on October 25, 2007 as DOI: 10.1124/dmd.107.017434
This article has not been copyedited and formatted. The final version may differ from this version.

PAMPA Data Analysis. The P_{app} and membrane retention (Rf) were determined using equations 4 and 5, respectively:

$$P_{app} = \frac{-2.303(V_A \cdot V_D)}{Area \cdot (t-\tau) \cdot (V_D + V_A)} \bullet \log\left\{1 - \frac{(V_D + V_A)}{(1-Rf) \bullet V_A} \bullet \frac{M_A(t)}{M_D(0)}\right\} \qquad 4$$

$$Rf = 1 - \left(\frac{M_D(t) + M_A(t)}{M_D(0)}\right) \qquad 5$$

Where V_A (ml) and V_D (ml) are the volumes of the acceptor and donor compartments, respectively, τ is the time to steady state (typically assumed to be ~1800 sec for convention), t is the timescale of the experiment (7200 sec) and Area is the area of the filter (in cm^2; for insert plate listed above, 0.24 cm^2). Mass is M, for acceptor (A) and donor (D).

P-gp ATPase Assay. The ATPase assay uses membrane preparations from insect SF9 cells expressing only human P-gp. In the ATPase assay, two ATP molecules are hydrolyzed with the transport of each substrate molecule by P-gp, resulting in the release of two inorganic phosphates into the reaction buffer. The level of inorganic phosphate was measured via a secondary colormetric reaction in which the phosphate reacts with ammonium molybdate to produce a blue color (Drueckes et al., 1995). The reactions were done using a 96-well format in reaction buffer (50 mM Mes, 2 mM ethylene glycol-bis (2-aminoethylether)-N,N,N',N'-tetraacetic acid (EGTA), 2 mM dithiothreitol (DTT), 50 mM potassium chloride, 5 mM sodium azide (pH adjusted to 6.8 with Tris). The reaction mixture included test drugs in 5% dimethyl sulfoxide (DMSO) vehicle, 8 μg human P-gp membranes (Gentest, Woburn, MA) and 1000 μM ATP magnesium salt. The incubation volume was 0.06 mL. Baseline activity was determined by incubations of

P-gp with inhibitor (100 μM sodium orthovanadate). The reactions were incubated at 37°C for 20 minutes and stopped by the addition of 0.03 mL of 10% sodium dodecyl sulfate (SDS). Two volumes (0.18 mL) of detection reagent (7 mM ammonium molybdate, 3 mM zinc acetate, 16% ascorbic acid, pH 5.0) were dispensed to each well. The color reaction proceeded for 20 minutes in a 37°C incubator. Ammonium molybdate reacted with inorganic phosphate to form a colorimetric complex. The plate was read immediately for end-point absorbance at 850 nm using a Safire plate reader (Tecan, Durham, NC). A potassium phosphate standard curve was used to extrapolate nanomoles of phosphate from the absorbance readings. ATPase activities were calculated in terms of nanomoles of phosphate per milligram of total vesicle protein per minute of incubation time. The substrate saturation model, Michaelis-Menten kinetics, was used to fit the dose-response data by nonlinear regression to obtain estimated apparent affinity values (Km) for ATPase enzyme.

Eight concentrations of each drug were evaluated in triplicate in two independent assays. Initially, test compounds were tested at concentration ranging between 1.25 μM and 150 μM, yet some compounds were retested using higher concentrations in order to saturate the ATPase enzyme. Estimated Km values were determined for those compounds exhibiting ATPase activity. Kinetics were not determined if no significant ATPase activity was observed.

Calcein-AM P-gp Inhibition Assay. Parental MDCK and MDR1-transfected MDCK cells were grown as described above. For the studies, each cell line (50,000 cells per well) was plated into Costar 3904 black 96 well plates (Packard Instrument Co., Meridian, CT)

with 100 µl medium supplemented with 1% FBS, and allowed to become confluent overnight. Test compounds were added to monolayers in 100 µl of culture medium containing 1% DMSO as solvent. Plates were incubated at 37^{o}C for 30 min. Calcein AM (Molecular Probes, Eugene, OR) was added in 100 µl of phosphate buffered saline (PBS) to yield a final concentration of 2.5 µM. Plates were incubated for another 30 min. Cells were then washed 3 times with ice cold PBS. PBS was added to the cells and the cells were read with a Victor fluorometer (Perkin Elmer, Downers Grove, IL) at excitation and emission wavelengths of 485 nm and 535 nm, respectively. P-glycoprotein inhibition was calculated using the following equation:

$$\%Inhibition = \frac{(The\,amount\,of\,inhibition)_{treated}}{(The\,amount\,of\,efflux)_{untreated}} \cdot 100$$

where "The amount of efflux" was defined as the fluorescence from MDCK cells subtracted by that from the MDR1-MDCK cells, and "The amount of inhibition" was $(\text{The amount of efflux})_{\text{untreated}}$ - $(\text{The amount of efflux})_{\text{treated}}$. The IC_{50} values were determined by fitting the percent of inhibition-concentration data into the Hill equation using the ordinary least square method of the LabStats Excel Add-in (Pfizer Inc.). When fitting the Hill Equation, cytotoxic data points for some compounds at the highest test concentration were removed. The cytotoxic data points were apparent because of the loss of calcein fluorescence at the highest test concentration of some compounds. The Hill slope, the minimum and the maximum % inhibition were not fixed, and the % inhibition data was not weighted. The IC_{50} was based on the concentration at which the apparent 50% inhibition was achieved (i.e., apparent IC_{50}). Vinblastine, a known inhibitor of P-gp was used as the positive control.

Results

Transwell Assay Results:

Transwell assays are used to measure drug movement through cell monolayers, and comparison of the ER determined in MDR1-MDCK versus MDCK cells (RR_{MDR1}) is a commonly used method to enable the assessment of whether a compound is a specific human P-gp substrate. Based on retrospective statistical analysis of inter-week variability of Pfizer transwell assay control data determined over one year (n > 280), a cutoff for RR_{MDR1} of 1.7 can be used to classify compounds as potential P-gp substrates (Pfizer data on file). A similar analysis was performed for transwell studies performed with Mdr1a-MDCK versus MDCK cells yielded a cutoff for RR_{Mdr1a} of 1.5. At Pfizer, the use of this cutoff has been demonstrated to minimize the incidence of false positives and negatives in this assay, as assessed by standard P-gp non-substrate, poor substrate and substrate controls (triprolidine, prazosin and quinidine, respectively).

Thirty-one CNS drugs and one active metabolite were identified for evaluation in transwell assays using human MDR1-MDCK, mouse Mdr1a-MDCK and MDCK cells, and the data are presented in table 1. Using 1.7 as a cutoff for the RR_{MDR1} and 1.5 as a cutoff for the RR_{Mdr1a}, 30 out of 32 compounds did not show positive efflux in both assays. Risperidone and its active metabolite, 9-OH risperidone, had RR_{MDR1} 2.0 and 3.3, and RR_{Mdr1a} 1.8 and 4.7, respectively. As such, these two compounds were identified as positive substrates for P-gp efflux for both human MDR1 and mouse Mdr1a using these assays.

Seven non-CNS drugs were measured in transwell assays using human MDR1-MDCK, mouse Mdr1a-MDCK and MDCK cells as well (Table 2). For the six reported P-

DMD Fast Forward. Published on October 25, 2007 as DOI: 10.1124/dmd.107.017434
This article has not been copyedited and formatted. The final version may differ from this version.

gp substrates of the seven non-CNS compounds: loperamide, prazosin, prednisone, quinidine, ritonavir and verapamil, RR_{MDR1} values were all above 1.7 and RR_{Mdr1a} values were all above 1.5, except for verapamil with RR_{Mdr1a} value of 1.4. RR_{MDR1} and RR_{Mdr1a} values for loratadine, which has been reported as a weak P-gp substrate in literature (Polli et al., 2001), were 0.5 and 0.6, respectively. Thus, loratadine was not identified as a P-gp substrate in both human and mouse P-gp assays.

P-gp ATPase assay results

The same set of compounds was examined for ATPase activity as well. A summary of estimated K_m of the CNS and non-CNS compounds was reported in table 1 and table 2, respectively. Kinetics were not determined if no significant ATPase activity was observed. Affinity of P-gp substrates are ranked as following: high affinity (K_m < 10 μM), moderate affinity (10 μM ≤ K_m < 50 μM) and low affinity (K_m ≥ 50 μM). Within the thirty-two CNS compounds, one compound, sertraline, had high affinity for human P-gp with K_m 9.4 μM, and four compounds: chlorpromazine, midazolam, paroxetine and risperidone, had moderate P-gp affinity with K_m values of 41.0 μM, 44.4 μM, 26.2 μM and 36.1 μM, respectively. Of the seven non-CNS compounds, loratadine and verapamil had high affinity for P-gp, loperamide, quinidine, and ritonavir had moderate affinity for P-gp, whereas the remaining two compounds were identified as low affinity or negative P-gp substrates.

Calcein AM P-gp inhibition assay

Calcein AM fluorescent assay can be used as a P-gp inhibition assay, and the inhibitors were ranked as the following: potent inhibitors (IC_{50} < 10 μM), moderate inhibitors (10 μM ≤ IC_{50} < 50 μM), and weak inhibitors (IC_{50} ≥ 50 μM). Of the thirty-two

CNS compounds the calcein AM assay indicated that haloperidol was a P-gp inhibitor with high potency (IC50 = 7.2 μM), buspirone, chlorpromazine, cyclobenzaprine, fluoxetine, hydroxyzine, paroxetine, and sertraline were identified as P-gp inhibitors with moderate potency, and the remaining compounds, including risperidone and 9-hydroxyrisperidone were weak P-gp inhibitors or did not exhibit P-gp inhibition (Table 1). Of the seven non-CNS compounds, loperamide and loratadine were P-gp inhibitors with high potency, quinidine and verapamil were P-gp inhibitors with moderate potency, and the remaining compounds were identified as weak P-gp inhibitors or did not exhibit P-gp inhibition (Table 2).

Permeability Measurements: PAMPA and MDCK A>B P_{app} Determinations

PAMPA is a high throughput passive permeability assay used to assess membrane permeability characteristics for compounds. Based on historical PAMPA data in Pfizer, compounds with PAMPA $P_{app} > 5 \times 10^{-6}$ cm/sec showed good membrane permeability characteristics in biological models such as Caco-2 and/or MDCK, whereas those with PAMPA $P_{app} < 5 \times 10^{-6}$ cm/sec may show membrane permeability liability. It should be noted that the cutoff of 5×10^{-6} cm/sec is a general value selected from empirical analysis of PAMPA vs. biology passive permeability data. Furthermore, we have observed that whereas 5×10^{-6} cm/sec is a general rule of thumb for predicting good membrane permeability, PAMPA P_{app} results can often be chemotype dependent, thus producing specific membrane permeability cutoffs for different chemotypes will be ideal. The membrane permeability of compounds was also tested in the WT MDCK as an alternate method to gauge compound passive P_{app} using a biological model. As mentioned previously, endogenous expression of transporters in MDCK cells is low and

therefore transmonolayer permeability is likely to be primarily mediated by passive processes. Indeed, for the compounds tested in MDCK assay, ER of unity was obtained for the majority and this lack of polarity confirms that transport across MDCK was passive. Magnitude of P_{app} ($x10^{-6}$ cm/sec) in MDCK can be qualitatively grouped by the following: high permeability ($P_{app} > 10$), moderate permeability ($1 \leq P_{app} \leq 10$), and low permeability ($P_{app} < 1$).

The permeability of the 32 CNS compounds was tested using PAMPA and MDCK assays (Table 3). PAMPA data suggested that fluoxetine and sulpiride, had very low permeability, and two compounds, morphine and sertraline, could be ranked as low permeability compounds as well, as judged by the empirical cutoff; whereas, the remainder showed good permeability. In the MDCK assay, only one compound, sulpiride, had low permeability, and other CNS compounds had moderate to high permeability. Passive permeability data for the seven non-CNS compounds is shown in table 4. Data from the two permeability assays indicated that all non-CNS compounds had moderate to high permeability.

DMD Fast Forward. Published on October 25, 2007 as DOI: 10.1124/dmd.107.017434
This article has not been copyedited and formatted. The final version may differ from this version.

DISCUSSION

This study assessed P-gp interactions with CNS and non-CNS drugs using different *in vitro* P-gp assay formats and passive permeability determination for these compounds. Our goal was to assess the ability of these *in vitro* studies in profiling P-gp efflux liability as it regards brain distribution. Thirty-one marketed CNS drugs, one active metabolite of a marketed CNS drug, plus seven non-CNS compounds, were tested in transwell assays using MDR1-MDCK, Mdr1a-MDCK, and MDCK cells, P-gp ATPase assay, Calcein AM P-gp inhibition assays, and compared with data generated *in vivo* from Mdr1a/Mdr1b (-/-/-/-) and WT mice (Doran et al., 2005). Conclusions from these studies were made in order to provide guidance for the interpretation of pre-clinical *in vitro* and *in vivo* P-gp models.

Each of the three *in vitro* P-gp assays have strengths and weaknesses as drug discovery screens to identify P-gp substrates and to assess the relevance of P-gp efflux liability *in vivo*. The advantage of the transwell assay is that it is cell-based, mimicking the *in vivo* conditions, and that it measures transport representative of processes underlying disposition. The MDCK cell line has the essential property of spontaneously forming polarized monolayers on solid supports with tight junctions, such that the efflux transporters can insert into the apical membrane to impart polarity to the transport of substrates (Cho et al., 1989). Polarity can be readily assessed via comparison of transport performed in B>A and A>B directions by determining the ER. Our studies in transwell assay employed three related cell lines (the parent MDCK, the human MDR1-transfected MDCK and the murine Mdr1a-transfected MDCK). Both transfectants produce high level of their respective transfected gene product and are presumed to express all other

MDCK specific canine renal transporters as well, such as dog P-gp, but at a much lower level than the transfected gene product. Given the homogenous nature of the screening panel, an MDCK background subtraction was intended to correct for the influence of transporters other than P-gp and underlies our rationale for performing studies in the WT MDCK cells in addition to the transporter-transfected MDCK cells. As such, by comparing the ER of compounds in the MDR1- or Mdr1a-transfected MDCK cells with the parent MDCK cells, the respective RR values can be used to positively identify a compound as a specific human or mouse P-gp substrate.

The P-gp ATPase assay estimates apparent affinity of the test compounds by measuring the level of inorganic phosphate, and can generate the apparent affinity of a compound (Km) for P-gp. The ATPase assay uses P-gp membrane preparations from insect cells, which could function differently from mammalian cells. The third P-gp *in vitro* assay, the Calcein AM P-gp inhibition assay, is able to identify P-gp inhibitors using a fluorescent probe substrate, but there is no necessary correlation between P-gp substrates and P-gp inhibitors, presumably due to multiple binding sites in P-gp. However, in comparison to the transwell assay, the P-gp ATPase assay and the Calcein AM P-gp inhibition assay are more cost effective, less labor intensive, and do not require an LC/MS/MS endpoint.

Data from transwell assays can be used to categorize compounds into three classes. The quantitative cutoffs have been established based on retrospective analysis of historical performance of efflux substrates in the *in vitro* assay and comparison with B/P ratios from Mdr1a/1b KO and WT mice. The first class is composed of non-transported compounds, i.e. the compound has no significant efflux (ER < 2.5) in both MDCK as

DMD Fast Forward. Published on October 25, 2007 as DOI: 10.1124/dmd.107.017434
This article has not been copyedited and formatted. The final version may differ from this version.

well as the MDR1-MDCK. The second class of compounds has RR_{MDR1} greater than 1.7 which is the hallmark for a positive human P-gp substrate. The third class of compounds has RR_{MDR1} less than 1.7, but there are individual effluxes (ER > 2.5) in MDR1-MDCK and MDCK, which are interpreted as having transporter activity, but not necessarily human MDR1 specific. The same criteria apply to results of studies performed with mouse Mdr1a-MDCK vs. MDCK, with the exception of 1.5 instead of 1.7 as a cutoff. Of the thirty-two CNS drugs, the transwell study data indicated that 94% of compounds had mean RR_{MDR1} and RR_{Mdr1a} values equal or less than 1.7 and 1.5, respectively, and these were classified as non-P-gp substrates. Only one CNS drug, risperidone (RR_{MDR1} 2.0) and its metabolite 9-OH risperidone (RR_{MDR1} 3.3), were identified as both human and mouse P-gp substrates using the RR_{MDR1} and RR_{Mdr1a} data interpretation criteria. The P-gp ATPase assay identified risperidone and 9-OH risperidone as a moderate and low affinity P-gp substrate with Km values as 36.1 μM and 177 μM, respectively. Consistent with data from the *in vitro* transwell studies, risperidone and 9-OH risperidone showed marked differences in B/P AUC ratios between P-gp KO and WT mice equal to 10 and 17, respectively (Doran et al., 2005). In addition, the brain concentration for metoclopramide was also dramatically increased in the P-gp KO mice (6.6-fold), and B/P between P-gp KO and WT mice for the three compounds were significantly greater than 4. A cutoff of 4 for B/P AUC ratios between P-gp KO and WT mice has been set to assess the P-gp interaction *in vivo*, after conducting a multivariate analysis of *in vivo* data for a population (n = 23) of Pfizer compounds with *in vitro* MDR1-MDCK data strongly indicative of non-substrates. The RR_{MDR1} and RR_{Mdr1a} data for metoclopramide generated from transwell assays was both 1.4, and the compound was identified as non-

DMD Fast Forward. Published on October 25, 2007 as DOI: 10.1124/dmd.107.017434
This article has not been copyedited and formatted. The final version may differ from this version.

P-gp substrate *in vitro*. Possibilities for this discrepancy could include interspecies differences in intrinsic activity of P-gp between human and mouse, or different expression levels at the BBB between the species. There is literature indicating that there is a species difference in P-gp substrates between human and mouse (Yamazaki et al., 2001). However, in the present studies, transwell data from MDR1-MDCK correlated well with that from Mdr1a-MDCK. In addition, we have previously tested 3300 Pfizer compounds in MDR1-MDCK and Mdr1a-MDCK transwell assays, and there was high correlation (R^2 = 0.92) for efflux ratios between human MDR1-MDCK and mouse Mdr1a-MDCK (Figure 1). Thus, species differences for P-gp between human and mouse is relatively rare, although it could be observed for a particular structural class of compounds. Another consideration is that there are two Mdr genes, 1a and 1b, in the mouse, although Mdr1a has been reported to be the major Mdr gene encoding mouse P-gp. *In vitro*, the compounds were only tested in the Mdr1a-MDCK assay, whereas, *in vivo* studies were done in the Mdr1a/Mdr1b double knockout mice. This may explain the difference between the *in vitro* and *in vivo* observations of metoclopramide. Additionally, it is important to note that the transfected cell lines possess approximately 4-fold more transporter activity relative to the endogenous canine P-gp activity in the parental MDCK. Consequently, the *in vitro* data may not necessarily reflect the magnitude of the *in vivo* effect. The definitive answer for the discrepancy of metoclopramide between *in vitro* and *in vivo* needs to be further investigated. Overall, compared with the *in vivo* B/P AUC ratios in P-gp KO and WT mice for the thirty-two CNS compounds, the transwell assay predicted no false positives, few false negatives (3%), and had a 97% correlation of *in vitro* versus *in vivo* data.

The seven non-CNS compounds tested were identified as human P-gp substrates using data from transwell studies except loratadine. Loratadine was not identified as a P-gp substrate *in vivo* based on the B/P in P-gp KO and WT (Doran et al., 2005), although loratadine has been reported as a weak P-gp substrate in literature (Polli et al., 2001). Interestingly, the ATPase assay identified loratadine as a P-gp substrate with a high affinity (Km = 1.4 μM). This disconnect could be due to the good passive permeability of loratadine, thus efflux in transwell assay does not have a large impact for this compound. But this certainly requires further investigation. In the work by Doran et al., 2005, the B/P AUC ratios between P-gp KO and WT for the seven compounds: loperamide, prazosin, prednisone, quinidine, ritonavir, verapamil and loratadine, were 9.3, 2, 2.3, 36, 1.2, 17 and 1.9, respectively. Only loperamide, quinidine, and verapamil had B/P ratios in KO/WT greater than the cutoff of 4, while loratadine, as well as prazosin, prednisone and ritonavir, was not statistically significant *in vivo*.

Collectively, the studies with thirty-two CNS and seven non-CNS drugs suggested that RR values generated from transwell studies using MDR1-MDCK and MDCK cells show a good correlation with B/P AUC ratios in P-gp KO vs. WT mice *in vivo* (Figure 2). All CNS compounds, except metoclopramide, fell in the two expected quadrants using 1.7 as a cutoff for RR in transwell assay, and 4 as a cutoff for B/P in KO/WT. It is expected that RR values can classify positives and negatives, but may not necessarily reflect the magnitude of the *in vivo* effect for these compounds. From these studies we conclude that there is a high utility of this *in vitro* approach as a means to profile P-gp liability that may be observed *in vivo*, and as such, this *in vitro* approach

provides a useful screen to cull compounds which can then be further assayed using the more resource intense *in vivo* studies.

Compared with transwell assay, the other two P-gp assays, ATPase and Calcein AM, generated both more false positives and more false negatives for the thirty-two CNS compounds (Figures 3a and 3b). Since the transwell is a cell-based assay, the efflux ratio will reflect the resultant interplay of the permeability of compounds and P-gp interaction, which is more reflective of the *in vivo* situation. It is possible that compounds, such as loratadine, which are positive in the ATPase, but are negative in the transwell assay because of their cell permeability. Whereas the third P-gp *in vitro* assay, Calcein AM P-gp inhibition assay, was used to identify P-gp inhibitors. Given the differences among the three P-gp *in vitro* assays, it is not a surprise that compared with the P-gp ATPase and the Calcein AM P-gp inhibition assays, the transwell assay correlated better with the *in vivo* P-gp KO and WT mice studies. We found that transwell assay is the most reliable for predicting the P-gp efflux liability *in vivo*, and that it is the method of choice for evaluating drug candidates. However, the P-gp ATPase and Calcein AM assays can be serve as specialized assays to understand kinetics and inhibition of CNS compounds, and can complement the transwell assay to better characterize and predict P-gp modulators *in vivo*.

In the development of CNS compounds, P-gp efflux liability is a key factor to assess, however the intrinsic permeability of a compound is also an important property to consider. Regardless of the level of P-gp efflux liability, a compound that is unable to cross cell membranes will not penetrate into the brain. Consequently, low passive permeability is a risk for brain penetration. For compounds that can cross membranes,

DMD Fast Forward. Published on October 25, 2007 as DOI: 10.1124/dmd.107.017434
This article has not been copyedited and formatted. The final version may differ from this version.

the relationship between the efflux and permeability is complex (Lentz et al., 2000), and their relationship in CNS penetration is not well understood. However, understanding the contribution of permeability versus efflux transport of a compound across the BBB is critical to the understanding and translation of P-gp interactions from *in vitro* to *in vivo* settings. We have utilized two *in vitro* permeability assays; the PAMPA and the MDCK, to assess the passive permeability of compounds. The PAMPA assay assesses the passive permeability of compounds across an artificial membrane. The MDCK cells contain low endogenous transporters and the apparent permeability is typically governed primarily by passive processes. According to their PAMPA or MDCK A>B P_{app} values (Table 3), all of the thirty-two CNS compounds were ranked as having moderate-to-high permeability, except for sulpiride, which is consistent with its high polar surface area, reported in Doran et al., 2005. In general, MDCK A>B P_{app} and PAMPA data correlated well despite the differences between the two systems.

Based on the *in vitro* transwell data and the *in vivo* B/P in P-gp K/O and WT mice for the thirty-two marketed CNS compounds, the majority of the CNS compounds included in this study did not exhibit P-gp efflux liability and had moderate-to-high passive permeability. We conclude that the transwell assay using MDR1-MDCK and MDCK is a valuable *in vitro* assay to evaluate human P-gp interaction with compounds targeting CNS. Additionally, we have reported a high correlation between MDR1-MDCK and Mdr1a-MDCK assays giving further confidence that the mouse model is a useful tool to predict P-gp activity in humans. We hereby recommend a multifaceted approach using *in vitro* P-gp and permeability assays, in concert with *in vivo* P-gp KO and WT mice, for the successful development of CNS drugs.

Acknowledgements: The authors would like to thank Drs. Bill J. Smith, Ronald S. Obach, Tristan S. Maurer, Angela C. Doran, Dennis Pereira, Theodore E. Liston and James G. Baxter for their advice and support of this project. We also would like to thank Dr. David Potter for the statistical analysis and Professor Piet Borst from Netherlands Cancer Institute for providing MDR1-MDCK cells.

REFERENCES

Ambudkar SV, Dey S, Hrycyna CA, Ramachandra M, Pastan I, and Gottesman MM (1999) Biochemical, cellular, and pharmacological aspects of the multidrug transporter. *Annu Rev Pharmacol Toxicol* **39:**361–398.

Avdeef A and Testa B (2002) Physiochemical profiling in drug research: a brief survey of the state-of-the-art of experimental techniques. *Cell Mol Life Sci* **59:**1681-1689.

Cho MJ, Thompson DP, Cramer CT, Vidmar TJ, and Scieszka JF (1989) The Madin Darby canine kidney (MDCK) epithelial cell monolayer as a model cellular transport barrier. *Pharm Res* **6:**71-77.

Doran A, Obach RS, Smith BJ, et al. (2005) The impact of P-glycoprotein on the disposition of drugs targeted for indications of the central nervous system: evaluation using the Mdr1a/Mdr1b knock out mouse model. *Drug Metab Dispos* **33:**165-174.

Drueckes P, Schinzel R, and Palm D (1995) Photometric microtitre assay of inorganic phosphate in the presence of acid-labile organic phosphates. *Anal Biochem* **230:**173-177.

Fromm MF (2000) P-glycoprotein A defense mechanism limiting oral bioavailability and CNS accumulation of drugs. *Int J Clin Pharmacol Ther* **38:**69-74.

Kansy M, Senner F, and Gubernator K (1998) Physicochemical high throughput screening: parallel artificial membrane permeation assay in the description of passive absorption processes. *J Med Chem* **41:**1007-1010.

Kerns EH (2001) High throughput physicochemical profiling for drug discovery. *J Pharm Sci* **90:**1838-1858.

Kerr KM, Sauna ZE, and Ambudkar SV (2001) Correlation between steady-state ATP hydrolysis and vanadate-induced ADP trapping in human P-glycoprotein. *J Biol Chem* **276:**8657-8664.

Lentz KA, Wring SA, Humphreys JE, and Polli JE (2000) Influence of passive permeability on apparent P-glycoprotein kinetics. *Pharm Res* **17:**1456-1460.

Liminga G, Nygren P, and Larsson R (1994) Microfluorometric evaluation of calcein acetoxymethyl ester as a probe for P-glycoprotein-mediated resistance: effects of cyclosporin A and its nonimmunosuppressive analogue SDZ PSC 833. *Exp Cell Res* **212:** 291-296.

Litman T, Zeuthen T, Skovsgaard T, and Stein WD (1997) Competitive, non-competitive and cooperative interactions between substrates of P-glycoprotein as measured by its ATPase activity. *Biochim Biophys Acta* **1361:**169-176.

Polli JE, Wring SA, Humphreys JE, Huang L, Morgan JB, Webster LO, and Serabit-Singh CO (2001) Rational use of in-vitro P-glycoprotein assays in drug discovery. *J Pharmacol Exp Ther* **299:**620-628.

Ramachandra M, Ambudkar SV, Chen D, Hrycyna CA, Dey S, Gottesman MM, and Pastan I (1998) Human P-glycoprotein exhibits reduced affinity for substrates during a catalytic transition state. *Biochemistry* **37:**5010-5019.

Sakardi B, Price EM, Boucher RC, Germann UA, and Scarborough GA (1992) Expression of the human multidrug resistance cDNA in insect cells generates a high activity drug-stimulated membrane ATPase. *J Biol Chem* **267:**4854-4858.

Scarborough GA (1995) Drug-stimulated ATPase activity of the human P-glycoprotein. *J Bioenerg Biomembr* **27:**37-41.

Schinkel AH, Wagenaar E, Mol CAAM, and van Deemter L (1996) P-glycoprotein in the blood-brain barrier of mice influences the brain penetration and pharmacological activity of many drugs. *J Clin Investing* **97:**2517-2524.

Schinkel AH (1999) P-glycoprotein, a gatekeeper in the blood-brain barrier. *Adv Drug Del Rev* **36:**179-194.

Sugano K, Hamada H, Machida M, Ushio H, Saitoh K and Terada K (2001) Optimized conditions of bio-mimetic artificial membrane permeation assay. *Int J Pharm* **228:**181-188.

Tiberghien F and Loor F (1996) Ranking of P-glycoprotein substrates and inhibitors by a calcein-AM fluorometry screening assay. *Anticancer Drugs* **7:**568-578.

Wohnsland F and Faller B (2001) High-throughput permeability pH profile and high-throughput alkane/water log P with artificial membranes. *J Med Chem* **44:**923-930.

Yamazaki M, Neway WE, Ohe T, Chen I, Rowe JF, Hochman JH, Chiba M, and Lin JH (2001) In vitro substrate identification studies for p-glycoprotein-mediated transport: species difference and predictability of in vivo results. J Pharmacol Exp Ther **296:**723-735.

Legend for figure:

Figure 1: Correlation of efflux ratio in transwell assays using mouse Mdr1a-MDCK and human MDR1-MDCK for 3300 Pfizer compounds. The y axis is the mouse Mdr1a-MDCK efflux ratio, and the x axis is the human MDR1-MDCK efflux ratio. R^2: 0.92. Solid line is the linear regression line, and the dotted line is the 95% prediction interval.

Figure 2: Correlation of ratio of ratios in transwell assay using MDR1-MDCK vs. MDCK cells with Brain/Plasma AUC ratios in Mdr1a/1b KO mice and FVB wild-type mice for the 32 CNS (O) and 7 non-CNS drugs (●). The dot lines indicate a cutoff of 4 for Brain/Plasma ratios between P-gp KO and WT mice, and a cutoff of 1.7 for ratio of ratios in MDR1-MDCK vs MDCK.

Figure 3: Correlation of P-gp ATPase Km (a) and calcein AM P-gp inhibition IC_{50} (b) with Brain/Plasma AUC ratios in Mdr1a/1b KO mice and FVB wild-type mice for the 32 CNS (O) and 7 non-CNS drugs (●). The dot lines indicate a cutoff of 4 for Brain/Plasma ratios between P-gp KO and WT mice, and a cutoff of 100 μM for P-gp ATPase Km and calcein AM P-gp inhibition IC_{50} to differentiate P-gp substrate vs. non-P-gp substrate and P-gp inhibitor vs. non-P-gp inhibitor. Compounds with negative Km values in ATPase assay were graphed in figure 3a with Km values of 500 μM, and compounds with IC_{50} higher than 100 μM were graphed in figure 3b with IC_{50} values of 200 μM.

TABLE 1

Transwell assays using MDR1-MDCK, Mdr1a-MDCK and MDCK cells, ATPase assay, Calcein AM P-gp inhibition assay, and Brain/Plasma AUC ratios in Mdr1a/1b (-/-, -/-) and FVB mice for 32 CNS-active compounds

Drugs	B/P in KO/WT[a]	MDR1-MDCK Efflux Ratio[b]	Mdr1a-MDCK Efflux Ratio[b]	MDCK Efflux Ratio[b]	Ratio of ratios in MDR1-MDCK/ MDCK	Ratio of ratios in Mdr1a-MDCK/ MDCK	ATPase Km (μM)[b]	Calcein IC50 (μM)
Buspirone	1.3	0.8 ± 0.11	0.6 ± 0.02	0.8 ± 0.14	1.0	0.8	118 ± 22.2	17.5
Caffeine	1.1	0.6 ± 0.07	0.6 ± 0.01	0.4 ± 0.29	1.4	1.5	neg	>100
Carbamazepine	1.1	0.7 ± 0.06	0.7 ± 0.06	0.8 ± 0.10	0.9	0.9	neg	>100
Carisoprodol	1.2	0.7 ± 0.03	0.7 ± 0.07	0.9 ± 0.15	0.8	0.8	neg	>100
Chlorpromazine	1.3	1.5 ± 0.49	1.8 ± 0.75	2.9 ± 1.34	0.5	0.6	41.0 ± 1.07	15.2
Citalopram	1.9	1.3 ± 0.27	1.0 ± 0.05	0.8 ± 0.19	1.6	1.2	441 ± 140.1	52.5
Cyclobenzaprine	1.4	0.5 ± 0.05	0.5 ± 0.02	0.6 ± 0.06	1.0	0.9	77.4 ± 26.86	18.7
Diazepam	1.2	0.7 ± 0.08	0.7 ± 0.05	0.9 ± 0.14	0.8	0.8	141 ± 38.0	100.5
Ethosuximide	1.0	0.8 ± 0.07	0.8 ± 0.03	0.9 ± 0.03	0.9	0.9	neg	>100
Fluoxetine	1.5	0.6 ± 0.06	0.7 ± 0.07	1.2 ± 0.12	0.5	0.6	51.6 ± 11.81	31.0
Fluvoxamine	2.3	0.7 ± 0.17	0.6 ± 0.12	0.8 ± 0.31	0.9	0.8	180 ± 35.7	>100
Haloperidol	1.4	0.8 ± 0.28	0.7 ± 0.25	1.0 ± 0.47	0.8	0.7	neg	7.2
Hydrocodone	2.1	0.9 ± 0.10	0.9 ± 0.05	0.8 ± 0.05	1.1	1.0	neg	>100
Hydroxyzine	1.0	0.6 ± 0.09	0.5 ± 0.09	0.8 ± 0.28	0.8	0.7	100 ± 42.7	19.1
Lamotrigine	1.0	0.7 ± 0.04	0.7 ± 0.03	0.8 ± 0.01	0.9	0.9	neg	>100
Methylphenidate	1.6	0.8 ± 0.06	0.8 ± 0.07	0.9 ± 0.10	0.9	0.9	neg	>100
Metoclopramide	6.6*	1.1 ± 0.27	1.1 ± 0.18	0.8 ± 0.18	1.4	1.4	neg	>100
Midazolam	1.0	0.7 ± 0.06	0.7 ± 0.08	0.8 ± 0.15	0.9	0.8	44.4 ± 5.06	>100
Morphine	1.7	1.7 ± 0.23	1.7 ± 0.31	1.4 ± 0.28	1.3	1.3	neg	>100
Nortriptylline	1.8	0.6 ± 0.03	0.5 ± 0.05	0.6 ± 0.03	1.1	0.9	56.0 ± 15.73	>100

Paroxetine	2.2	0.7 ± 0.02	0.7 ± 0.07	0.7 ± 0.01	1.0	1.0	26.2 ± 1.02	27.5
Phenytoin	1.2	0.9 ± 0.09	0.8 ± 0.03	0.9 ± 0.08	1.0	0.9	neg	>100
Propoxyphene	2.6	0.7 ± 0.14	0.6 ± 0.07	0.7 ± 0.17	1.0	0.9	180 ± 67.5	63.3
Risperidone	10*	1.2 ± 0.36	1.1 ± 0.19	0.6 ± 0.30	**2.0**	**1.8**	36.1 ± 1.23	70.7
9-OH Risperidone	17*	2.1 ± 0.18	3.0 ± 0.20	0.6 ± 0.31	**3.3**	**4.7**	177 ± 1.2	>100.
Selegiline	1.1	0.8 ± 0.08	0.8 ± 0.04	0.9 ± 0.14	0.8	0.8	neg	>100
Sertraline	1.1	3.6 ± 0.42	5.4 ± 0.56	10.0 ± 1.09	0.4	0.5	9.4 ± 1.45	30.0
Sulpiride	1.9	0.9 ± 0.59	2.7 ± 1.62	2.0 ± 0.74	0.5	1.4	neg	>100
Thiopental	1.2	0.9 ± 0.07	0.8 ± 0.03	0.9 ± 0.08	1.0	0.9	neg	>100
Trazodone	0.9	0.8 ± 0.03	0.7 ± 0.07	0.8 ± 0.11	0.9	0.9	172 ± 44.5	>100
Venlafaxine	1.8	0.6 ± 0.02	0.7 ± 0.03	0.7 ± 0.01	0.9	1.0	neg	>100
Zolpidem	1.4	0.7 ± 0.06	0.6 ± 0.04	0.7 ± 0.06	1.0	0.9	198 ± 1.0	>100

[a] *The data for B/P in P-gp KO/WT mice were extracted from Doran et al., 2005*

[b] *Data are presented as mean ± SD*

** P < 0.05, probability of KO/WT ratio > 4.*

Neg., no stimulation of ATPase activity

Table 2

Transwell assays using MDR1-MDCK, Mdr1a-MDCK and MDCK cells, ATPase assay, Calcein AM P-gp inhibition assay, and B/P AUC ratios in Mdr1a/1b (-/-, -/-) and FVB mice for 7 non-CNS drugs

Compound	B/P in KO/WT [a]	MDR1-MDCK Efflux Ratio[b]	Mdr1a-MDCK Efflux Ratio[b]	MDCK Efflux Ratio[b]	Ratio of ratios in MDR1-MDCK/ MDCK	Ratio of ratios in Mdr1a-MDCK/ MDCK	ATPase Km (μM)[b]	Calcein IC50 (μM)
Loperamide	9.3*	9.4 ± 4.08	7.1 ± 2.70	2.5 ± 1.31	**3.8**	**2.9**	11.4 ± 0.22	4.9
Loratadine	1.9	0.9 ± 0.35	1.0 ± 0.46	1.8 ± 1.18	0.5	0.6	1.4 ± 0.90	7.5
Prazosin	2.0	3.2 ± 0.61	3.3 ± 0.77	1.1 ± 0.22	**2.9**	**3.1**	54.6 ± 3.00	>100
Prednisone	2.3	3.8 ± 0.88	3.4 ± 0.74	1.3 ± 0.34	**2.8**	**2.5**	291 ± 9.9	>100
Quinidine	36*	16.1 ± 4.40	14.3 ± 5.25	2.2 ± 0.65	**7.4**	**6.6**	13.7 ± 2.71	30.2
Ritonavir	1.2	49.5 ± 29.65	64.4 ± 21.5	2.7 ± 0.20	**18.4**	**23.9**	11.3 ± 1.16	63.5
Verapamil	17*	1.8 ± 0.10	1.2 ± 0.22	0.8 ± 0.20	**2.1**	1.4	9.0 ± 0.38	18.1

[a] *The data for B/P in P-gp KO/WT mice were extracted from Doran et al., 2005*

[b] *Data are presented as mean ± SD*

** P < 0.05, probability of KO/WT ratio > 4*

Table 3

P_{app} in PAMPA and $P_{app,A>B}$ values in MDCK for 32 CNS-active drugs

Compound	PAMPA Retention Factor (RF)[a]	PAMPA P_{app} ($X10^{-6}$ cm/sec)[a]	$P_{app,A>B}$ in MDCK ($X10^{-6}$ cm/sec)[a]
Buspirone	0.5 ± 0.04	27.1 ± 19.95	23.3 ± 3.91
Caffeine	N.D.	N.D.	30.6 ± 2.47
Carbamazepine	0.2 ± 0.05	17.3 ± 2.38	29.4 ± 2.46
Carisoprodol	0.2 ± 0.06	16.2 ± 2.57	25.6 ± 2.86
Chlorpromazine	0.9 ± 0.03	6.1 ± 1.64	4.1 ± 0.44
Citalopram	0.5 ± 0.04	14.5 ± 3.74	18.3 ± 3.76
Cyclobenzaprine	0.8 ± 0.04	13.0 ± 2.49	12.2 ± 0.34
Diazepam	0.5 ± 0.03	17.4 ± 3.18	27.7 ± 2.45
Ethosuximide	0.1 ± 0.12	10.0 ± 1.24	26.8 ± 2.59
Fluoxetine	0.3 ± 0.08	0.1 ± 0.03	6.3 ± 0.61
Fluvoxamine	0.8 ± 0.06	10.0 ± 0.35	13.0 ± 2.69
Haloperidol	0.8 ± 0.04	8.6 ± 1.30	12.3 ± 3.31
Hydrocodone	0.2 ± 0.08	11.9 ± 0.25	20.0 ± 1.77
Hydroxyzine	0.6 ± 0.01	12.5 ± 0.56	16.1 ± 3.25
Lamotrigine	N.D.	N.D.	22.9 ± 0.97
Methylphenidate	0.3 ± 0.04	23.2 ± 6.53	24.7 ± 2.03
Metoclopramide	0.4 ± 0.05	11.0 ± 1.27	17.7 ± 2.61
Midazolam	0.5 ± 0.02	13.1 ± 1.28	22.5 ± 2.08
Morphine	0.2 ± 0.05	4.8 ± 0.78	1.8 ± 0.07
Nortriptylline	0.8 ± 0.06	10.1 ± 2.51	9.1 ± 0.16
Paroxetine	0.9 ± 0.01	5.7 ± 1.08	6.1 ± 0.29
Phenytoin	0.3 ± 0.03	15.2 ± 0.63	24.0 ± 1.80
Propoxyphene	0.6 ± 0.04	13.1 ± 1.08	21.9 ± 4.65

Risperidone	0.5 ± 0.05	13.8 ± 0.50	19.8 ± 3.24
9-OH Risperidone	N.D.	N.D.	16.8 ± 1.04
Selegiline	0.6 ± 0.04	26.1 ± 11.91	23.2 ± 1.46
Sertraline	0.9 ± 0.02	2.8 ± 0.50	1.9 ± 0.37
Sulpiride	0.01 ± 0.01	0.03 ± 0.03	0.9 ± 0.47
Thiopental	0.5 ± 0.02	21.1 ± 6.39	25.2 ± 1.15
Trazodone	0.5 ± 0.03	13.6 ± 1.07	19.7 ± 0.64
Venlafaxine	N.D.	N.D.	22.1 ± 0.77
Zolpidem	0.4 ± 0.03	15.7 ± 1.45	23.4 ± 0.76

N.D., no data was generated.

[a] *Data are presented as mean ± SD*

Table 4

P_{app} in PAMPA and A>B P_{app} values in MDCK for 7 non- CNS drugs

Compound	PAMPA Retention Factor (RF)[a]	PAMPA P_{app} ($X10^{-6}$ cm/sec)[a]	A>B P_{app} in MDCK ($X10^{-6}$ cm/sec)[a]
Loperamide	0.8 ± 0.02	7.8 ± 0.66	2.7 ± 1.07
Loratadine	1.0 ± 0.01	5.0 ± 1.35	8.9 ± 3.70
Prazosin	0.4 ± 0.10	9.9 ± 0.53	10.6 ± 1.67
Prednisone	0.3 ± 0.03	11.2 ± 0.42	12.3 ± 1.83
Quinidine	0.4 ± 0.04	12.9 ± 1.65	8.0 ± 1.91
Ritonavir	N.D.	N.D.	5.6 ± 0.58
Verapamil	0.6 ± 0.01	11.5 ± 0.60	12.6 ± 1.83

N.D., no data was generated

[a] *Data are presented as mean ± SD*

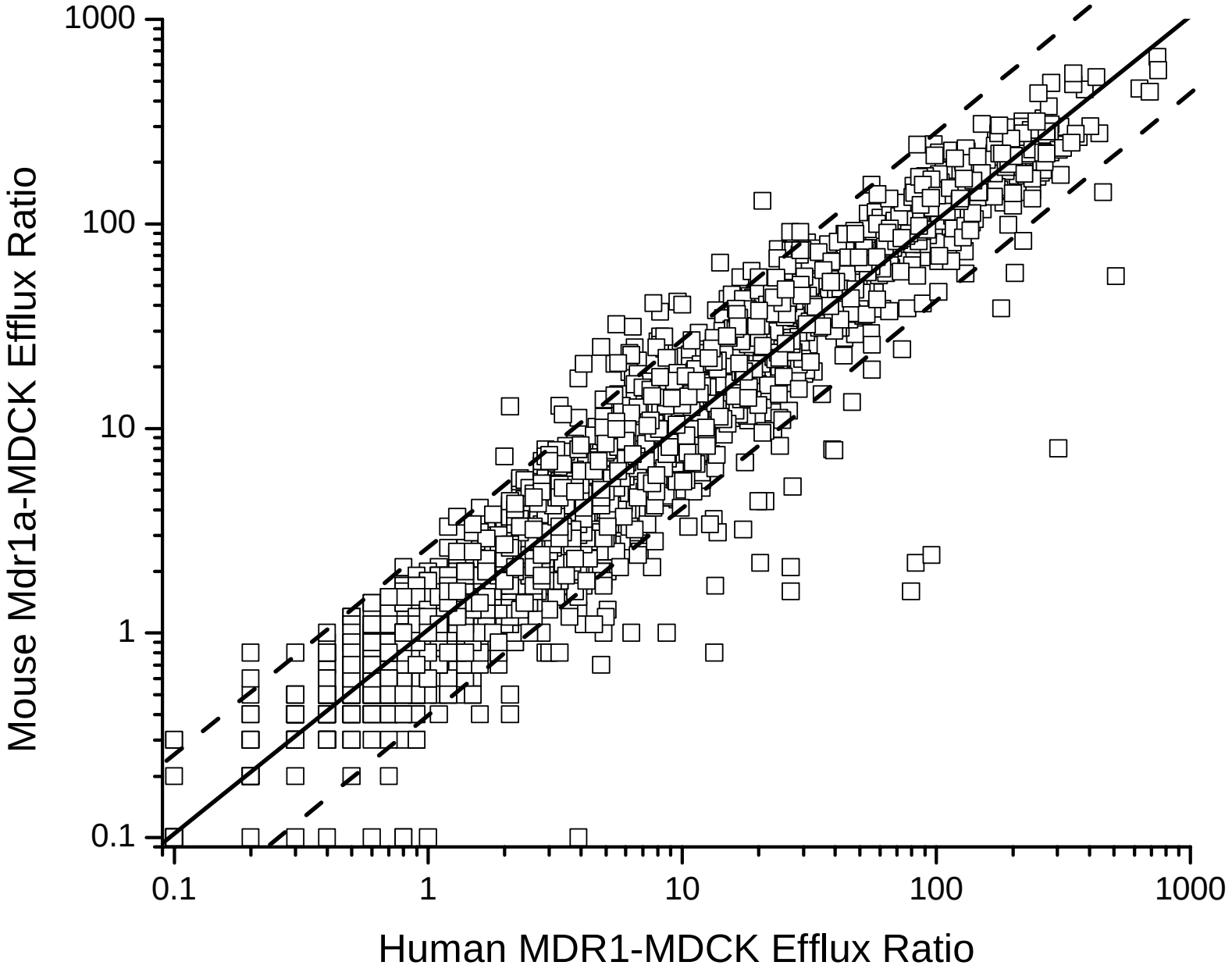

Fig.1

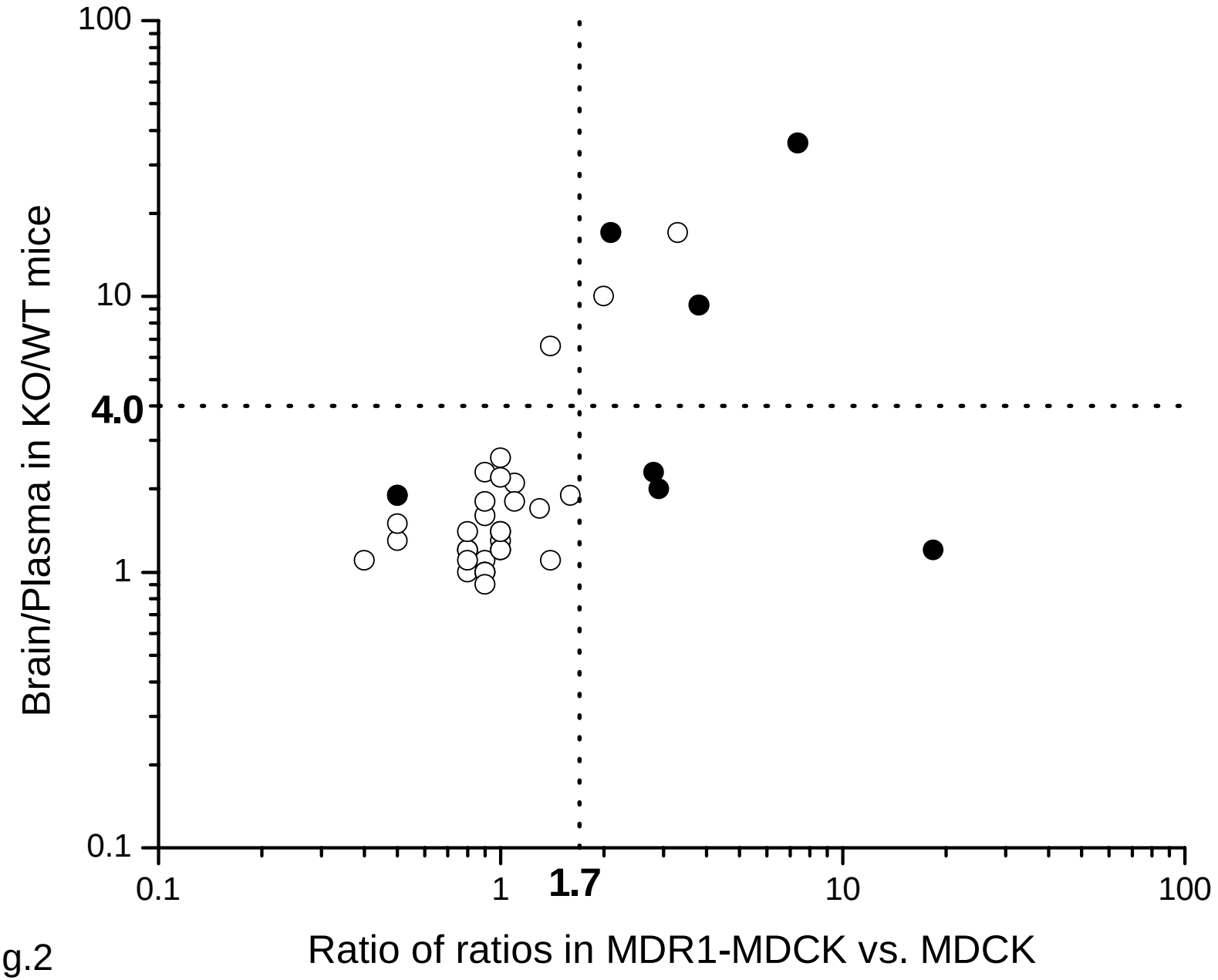

Fig.2

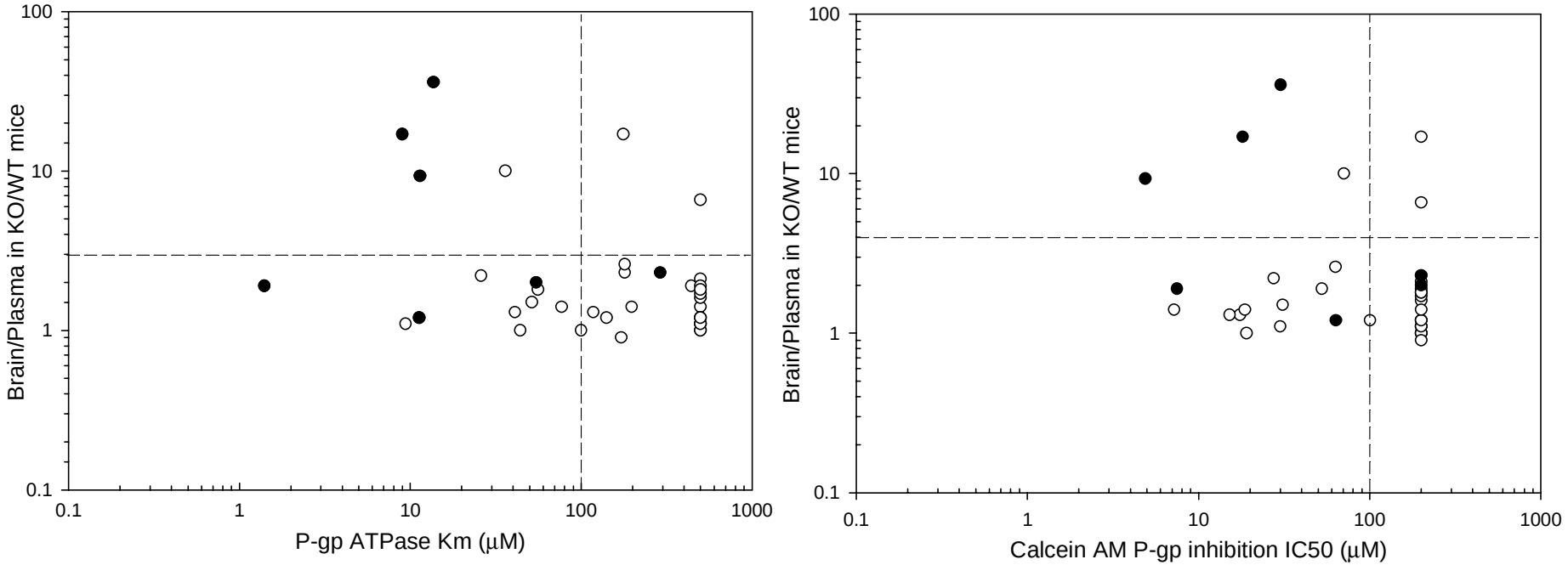

Fig 3a and 3b